Journal of Applied Fluid Mechanics, Vol. 17, No. 9, pp. 1874-1884, 2024.
Available online at www.jafmonline.net, ISSN 1735-3572, EISSN 1735-3645.
https://doi.org/10.47176/jafm.17.9.2572

Influence of a Modified Weir Profile on Velocity Field and Dissipation Rate in Stepped Spillways: A Comparative Study Using Physical Models and Computational Fluid Dynamics

H. Souli†, J. Ahattab and S. Bensallam

Hydraulic, environmental, marine, soil and structural systems, Hassania School of public works Casablanca, Morocco

†*Corresponding Author Email: Souli.hamza.cedoc@ehtp.ac.ma*

ABSTRACT

Stepped spillways are specialized hydraulic structures crafted to optimize the effective dissipation of hydraulic energy along stepped chutes. The central objective is to scrutinize and improve the mitigation of flow separation occurring from the ogee crest to the stepped chute, focusing on various profiles within the critical zone (CZ) to understand its flow behavior. The study evaluates the impact of CZ profile alterations on velocity distribution, revealing a reduction in velocity ranging from 10% to 18% for nappe flow and 7% to 15% for skimming flow, with a dissipation rate 5% higher than other tested profiles in the CZ. By combining physical experiments and numerical simulations, the research aims to understand the complex dynamics of CZ flow. A comparative analysis is conducted, comparing turbulence models (specifically RNG) against experimental data for velocity and dissipation rate, considering different numbers of steps (N=16, 22, 56, 60). Moreover, the research seeks to unravel the effects of introducing additional steps within the CZ on crucial hydraulic parameters. The results indicate a significant improvement in flow patterns, velocity fields, and energy dissipation for the modified profile, highlighting the practical applicability of the proposed approaches in effectively sizing the CZ.

Article History

Received January 4, 2024
Revised April 7, 2024
Accepted April 9, 2024
Available online July 2, 2024

Keywords:

Spillways
Hydraulic of dams
Stepped spillways
Computational fluid dynamics
Turbulence modelling
Transition zone

1 INTRODUCTION

Spillways constitute crucial and substantial elements within the flood evacuation systems of dams, representing a significant investment. The effective functioning of a spillway hinges on the optimal design of all its components.

The stepped spillway assumes a pivotal function in flood control, notably for recently constructed dams using Roller-Compacted Concrete (RCC). Integral to the hydraulic system of the dam, this spillway adeptly oversees and modulates water flow during heightened discharge periods. Its structured design enables controlled energy dissipation, effectively reducing erosion risks and enhancing flood control measures.

Stepped spillways with solid steps are hydraulic structures that allow high rate of dissipation in comparison with the smooth ones.

Recently, a study by (Daneshfaraz et al., 2024a) was undertaken to investigate the effects of rough steps on stepped spillways in relation to energy dissipation and hydraulic jumps. The findings revealed that rough steps outperform smooth steps in terms of energy dissipation, particularly for the nappe flow regime.

In general, stepped spillways are composed of three main parts: the ogee crest, the stepped chute with height h and length l and the stilling basin that dissipate the residual energy in the bottom of the stepped chute (Rajaratnam, 1990; Chanson, 2001; Boes & Hager, 2003a; AlTalib et al., 2019; Hager et al., 2020).

On the other hand, stepped Gabion steps on stepped spillways represent a potentially viable alternative to solid impermeable steps, offering economic advantages, ease of implementation, and stability through the reduction of water pressure, leading to effective energy dissipation. Daneshfaraz et al. (2024b) conducted a study to investigate hydraulic jumps and the rate of energy dissipation downstream of gabion stepped spillways under various flow regimes.

The flow behavior of stepped spillways differs significantly from classic smooth spillways by:

NOMENCLATURE

y_c	critical depth	V_F	fractional volume
f_b	friction factor	R_{DIF}	turbulent diffusion
$D_{h,w}$	hydraulic diameter	R_{SOR}	mass source term
h_w	clear water depth of flow with reference to the pseudo-bottom	f	viscous acceleration
$K_s = h\cos(\theta)$	step roughness	b	flow losses
$h_{w,u}$	water level at the uniform conditions of the flow	P_T	transport equation for turbulent kinetic energy
C	discharge coefficient	G_T	buoyancy production
L	length of the weir	$Diff_T$	diffusion term
H	head discharge above the weir	$H\text{-}k-\varepsilon$	head discharge derived using $k-\varepsilon$
$H\text{-}RNG\ k-\varepsilon$	head discharge derived using $RNG\ k-\varepsilon$	*H-Emp*	head discharge derived using empirical calculations
H-Exp	head discharge measured using experimental data	χ	energy dissipation
y_1, y_2	conjugate depths	F	Froude number
h_w	clear water depth	H_{res}	residual energy
K_t	kinetic energy	H_{max}	maximum head discharge
ε_t	dissipation rate	V_F	fractional volume
q	unit flowrate	Q	volumetric flowrate

Nappe flow involves hydraulic jumps forming at each step, increasing energy dissipation. Transition flow is marked by pressure fluctuations and instability, and is generally not suitable for sizing the structure. Skimming flow has high velocity and creates a pseudo layer parallel to the slope of the stepped chute. For small water discharges, there may be spraying on horizontal steps, potentially causing damage to the entire structure.

The designers of these hydraulic structures try to deal with the problem of joint between the two regions by using several methods. Their aim is that the water surface of the flow stay attached to the surface in the transition zone and not causes any damage in this sensitive part of the dam.

An insertion of steps right after the tangential point T is unsuitable, so the idea is to add steps on the ogee crest before the tangential point, in order to avoid the problem of the creation of the thin film on the first horizontal step. This solution creates a spray zone for small discharges. Therefore, to counter the intensification of this zone downstream the tangential point a weir profile is proposed by CEDEX laboratory. The design head H is used for the conception of this transition zone (see Fig. 1).

Despite this design concept, experimental observations reveal that the issue of the spray zone persists. However, it is noteworthy that this concern arises not at the initial stages of the transition but specifically between the stepped weir and the stepped chute. To tackle these issues, this paper proposes to add more small steps to the initial profile developed by CEDEX (Mateos Iguacel & Elviro Garcia, 1995)

This study introduces a novel approach by extending the length of tangential point T, which effectively stabilizes the flow and prevents the formation of a new spray zone. This design of the crest ensures favorable

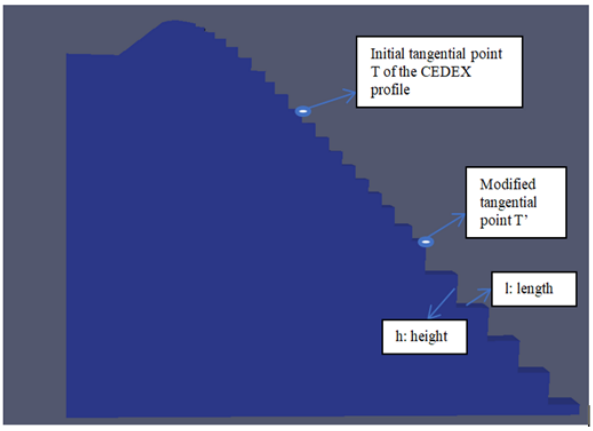

Fig. 1 Proposed profile in the transition zone

conditions, even under high flow discharges, and optimizes energy dissipation by ensuring continuous flow attachment with the steps, thereby mitigating the risk of cavitation and erosion and scouring as mentioned by (Ghaderi et al., 2020) downstream of the spillway.

The efficiency of the proposed profile was proved using both physical and numerical solutions.

Several studies have pursued similar objectives. Daneshfaraz et al. (2014) conducted a numerical study of the flow over stepped and ogee spillways using the finite element method. They compared two discretization methods in the numerical results and then compared these results with experimental data, finding a significant agreement between the two approaches.

Numerous researchers (Dalili Khanghah & Kavianpour, 2020) have examined the dissipation rate of stepped spillways, with recent focus on investigating the critical zone (CZ).

Notably, explored the influence of altering the shape of CEDEX on water surface behavior and flow patterns. Consequently, this paper aims to investigate the effects of modifying the CZ form on hydraulic parameters, including velocity field and dissipation rate. Employing a comprehensive approach, we employ experimental, numerical, and empirical.

2 MATERIALS AND METHODS

2.1 Modified Profile in the Transition Zone

To solve the problem of broad effect in the transition zone we have modified the CEDEX profile, by adding 6 to 9 new steps with the length of $\frac{H_{\max}}{6}$ (Hmax is the head discharge above the weir) starting from the initial tangential point T to the modified tangential point T'.

The Fig. 1 gives the hydraulic parameters of the modified profile.

Our objective is to introduce additional smaller steps to the water surface to reduce the impact of the spray zone, which has the potential to inflict actual harm to dam structures and create negative pressure. Following the T' tangency point, we have connected a fixed stepped chute with a designed height (h) and length (l).

2.2 Dissipation Rate

To estimate the energy dissipation we will use the empirical formula from (Boes & Hager, 2003a, b) ??? from several tests in the physical models:

The energy dissipation is the ratio between the maximal energy head above the ogee crest $H_{\max}$ and the residual energy H_{res} .

Energy dissipation can be obtain*ed using the Eq.1:*

$$\chi = \frac{H_{\max} - H_{res}}{H_{\max}} \tag{1}$$

$H_{\max}$ is equal to H_{dam} +1.5 y_c and the critical depth is estimated by Eq. 2:

$$y_c = (\frac{q^2}{g})^{\frac{1}{3}} \tag{2}$$

The Equation 3 gives the residual head H_{res} above the pseudo bottom:

$$H_{res} = z + h_w \cos(\theta) + 1.1\frac{q^2}{2gh_w} \tag{3}$$

Under conditions of uniform flow, (Takahashi et al., 2001) formulated an empirical formula for the energy loss at the toe of the stepped spillway with skimming flow regime given by the Eq. (4) (Takahashi et al., 2001; Ohtsu et al., 2004).

This formula remains applicable irrespective of the uniformity of the flow:

$$\chi = 1 - \frac{(\frac{h_w}{y_c})^{-2} + 2(\frac{h_w}{y_c})\cos(\theta)}{3 + 2\frac{H_{dam}}{y_c}} \tag{4}$$

For less $\frac{H_{dam}}{y_c}$ than 15 to 20:

We can determine the ratio of $\frac{H_{dam}}{H_{res}}$ using the Eq. (5):(Boes & Hager, 2003b, 2003c)

$$\frac{H_{res}}{H_{\max}} = \exp\left[(-0.045(\frac{K_s}{D_{h,w}})^{0.1}\sin(\theta)^{-0.8}\frac{H_{dam}}{y_c}\right] \tag{5}$$

For less $\frac{H_{dam}}{y_c}$ superior the 15 to 20, the normalized residual head is given by the Eq. (6):

$$\frac{H_{res}}{H_{\max}} = \frac{F}{\frac{H_{\max}}{y_c} + F} \tag{6}$$

The value of parameter F can be computed using the provided in the Eq. (7):

$$F = (\frac{f_b}{8\sin(\theta)})^{\frac{1}{3}}\cos(\theta) + \frac{\alpha}{2}(\frac{f_b}{8\sin(\theta)})^{\frac{-2}{3}} \tag{7}$$

2.3 Experimental Configurations

The investigation in this study is conducted through experimentation using a three-dimensional physical model to explore the effects of 3D conditions and gain comprehensive insights into flow behavior as shown in the Fig. 2. (Chanson & Gonzalez, 2005; Boes, 2020)

The experimental setup comprises the following components:

- The upstream section is a rectangular basin measuring (5m *7m).
- The downstream section, also a rectangular basin, is designed to investigate scour-related issues; however, this aspect is beyond the scope of the current article.

In the downstream section, a control gate is implemented to regulate the water level within the control section. This water level holds significant importance in capturing the hydraulic jump within the stilling basin.

The instrumentation employed in this study encompasses a Rolling point instrument characterized by high accuracy, with a sensitivity of ±0.001 m, utilized for measuring flow height above the weir. Additionally, a Magnetic flow meter with a sensitivity of ±0.001\% is employed to measure the flow rate.

Furthermore, a Pitot tube is utilized for velocity measurement, offering a sensitivity of ±0.02\% m/s. These precision instruments collectively contribute to accurate and reliable data collection for the assessment of hydraulic parameters in the experimental setup.

Fig. 2 Physical model

Table 1 Summary of tested cases

Hdam	h(m)	l(m)	N	Q(l/s)
1.44	0.06	0.048	56-60	10-83
0.5	0.02	0.03	16-22	

The Table 1 presents the properties and characteristics of the examined cases in the physical model.

Different flow discharges were tested (Q=10-83 l/s) ranging from (nappe flow to skimming flow). Samples of the laboratory data will be given in comparison with the numerical approaches for each part of the present research.

In order to investigate the flow patterns, a model was built as shown in the Fig. 2. This model facilitates the visualization of flow behavior for three profiles tested in the CZ: the initial design without transitional steps, the CEDEX profile, and a modified profile. In the first option, the crest profile was joined to the stepped chute without having any transitional steps. Problems were observed in terms of the behavior of the jet after hitting the first horizontal step, same outcomes were established by (Dalili Khanghah & Kavianpour, 2020).

In the second test, we clearly observe for small discharges in the physical model the same problem but this time after some steps.

Finally, for the modified profile we have chosen to increase the length of the tangential point in order to moderate this spray zone and to prevent damage namely cavitation (Regan et al., 1979; Quintela, 1980; Khatsuria, 2004; Baylar et al., 2006)that can be caused by the impingements of the jet.

2.4 Numerical Solution and Flow Simulation

Computational fluid dynamics (CFD) is an approach used to simulate fluid flow processes. It involves discretizing the well-known Navier-Stokes equations for fluid flow and the mass continuity equation, solving them for each computational cell (Tannehill et al., 1997).

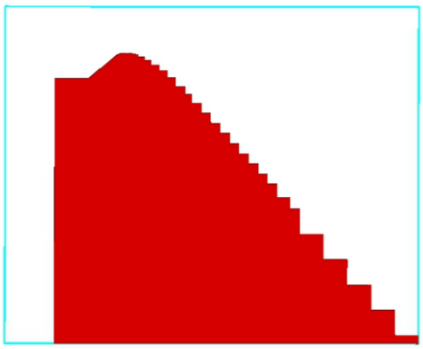

Fig. 3 Example of Tested Profile with number of 16 steps

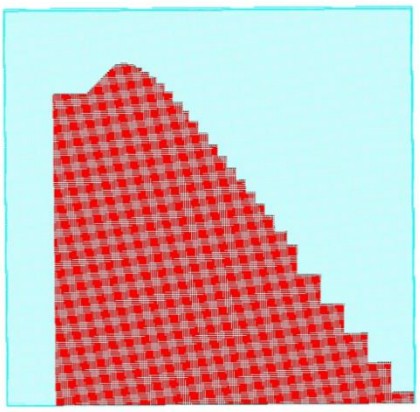

Fig. 4 Grid configurations

While Flow-3D stands out as prominent and robust software, plethora of other viable CFD tools and software options exists. For our study, we selected suitable CFD software to model the complex flow behavior within the (CZ) encompassing the stepped ogee crest and stepped chutes. Subsequently, we employed this software to compute the energy dissipation within this zone and compare these results against our experimental data. This comparison was undertaken to validate the accuracy and reliability of our numerical solution.

2.5 Meshing Analysis

For the geometric modeling, FreeCAD software was utilized to define the shape of the weir, as well as certain steps within the stepped chutes as illustrated in Fig. 3. Additionally, the software was employed to create a comprehensive model of the entire stepped spillway, facilitating the estimation of energy dissipation within the system.

A grid convergence analysis was conducted for each case study as shown in the Fig. 4, varying the mesh size from coarse to fine (2cms to 4 mm), to determine the appropriate cell size. The results of the grid convergence study in Tables 2, 3 indicate that, for CZ and the entire structure, the optimal cell size is determined to be 4 mm.

In our model, we selected a time step of 0.0001 seconds to address stability concerns. Each simulation extends duration of 100 seconds to attain a steady-state regime. The simulation process varied in duration,

Table 2 Grid analysis-CZ

	Ogee crest without steps	*N=16 steps*	N=22 steps
Cell size	2cms-1cm-4mm	2cms-1cm-4mm	2cms-1cm-4mm
Total number of cells	1 000 250	980 000	820 026

Table 3 Complete configuration of the stepped spillway

	Ogee crest without steps	*N=56 steps*	N=60 steps
Cell size	2cms-1cm-4mm	2cms-1cm-4mm	2cms-1cm-4mm
Total number of cells	15 020 533	14 825 666	14 222 236

ranging from 10 hours to several days for each case, encompassing the transition from nappe flow to skimming flow.

2.6 Turbulence Modeling and Water Surface Tracking

In most engineering applications, RANS model (Reynold averaged Navier-stokes equations) is used in order to model turbulence.

The mass continuity equation can be expressed in a general form as follows Eq. (8) (Pletcher et al., 1997; Kaheh et al., 2014; Bayon et al., 2016):

$$V_F \frac{\partial \rho}{\partial t} + \frac{\partial}{\partial x}(\rho u A_x) + R\frac{\partial}{\partial y}(\rho v A_y) + \frac{\partial}{\partial z}(\rho w A_z) + \xi \frac{\rho u A_x}{x} = R_{DIF} + R_{SOR} \quad (8)$$

The Equations (9), (10) provide the mass source term and the turbulent diffusion.

$$R_{DIF} = \frac{\partial}{\partial x}(\nu_p A_x \frac{\partial \rho}{\partial x}) + R\frac{\partial}{\partial y}(\nu_p A_y \frac{\partial \rho}{\partial y}) + \frac{\partial}{\partial z}(\nu_p A_z \frac{\partial \rho}{\partial z}) + \xi \frac{\rho \nu_p A_x}{x} \quad (9)$$

$$\frac{V_P}{\rho c}\frac{\partial P}{\partial t} + \frac{\partial u A_x}{\partial x} + R\frac{\partial v A_y}{\partial y} + \frac{\partial w A_z}{\partial z} + \xi \frac{u A_x}{x} = \frac{R_{SOR}}{\rho} \quad (10)$$

The momentum equations in three dimensions can be expressed as follows Eqs. (11), (12), (13):

$$\frac{\partial u}{\partial t} + \frac{1}{V_F}(u A_x \frac{\partial u}{\partial x} + \nu A_y \frac{\partial u}{\partial y} + w A_z \frac{\partial u}{\partial z}) - \xi \frac{A_y v^2}{x V_F} = -\frac{1}{\rho}\frac{\partial P}{\partial x} + G_x + f_x - b_x + \frac{R_{SOR}}{\rho V_F}(u - u_w - \delta u_s) \quad (11)$$

$$\frac{\partial v}{\partial t} + \frac{1}{V_F}(u A_x \frac{\partial v}{\partial x} + \nu A_y \frac{\partial v}{\partial y} + w A_z \frac{\partial v}{\partial z}) - \xi \frac{A_y u v}{x V_F} = -\frac{1}{\rho}(R\frac{\partial P}{\partial y}) + G_y + f_y - b_y + \frac{R_{SOR}}{\rho V_F}(v - v_w - \delta v_s) \quad (12)$$

$$\frac{\partial w}{\partial t} + \frac{1}{V_F}(u A_x \frac{\partial w}{\partial x} + \nu A_y \frac{\partial w}{\partial y} + w A_z \frac{\partial w}{\partial z}) = -\frac{1}{\rho}(\frac{\partial P}{\partial z}) + G_z + f_z - b_z + \frac{R_{SOR}}{\rho V_F}(w - w_w - \delta w_s) \quad (13)$$

For simulations, we utilized the RANS equations ($k-\varepsilon$, and RNG $k-\varepsilon$) see Eqs. (14), (15) in order to close the system and obtain the algebraic equations using finite volume approach.

They consist of two transport Eqs. (14), (15) for the turbulent kinetic energy (k_T) and its dissipation (ε_T), which are:

$$\frac{\partial k_T}{\partial t} + \frac{1}{V_F}(u A_x \frac{\partial k_T}{\partial x} + \nu A_y \frac{\partial k_T}{\partial x} + w A_z \frac{\partial k_T}{\partial z}) = P_T + G_T + Diff_T - \varepsilon_T \quad (14)$$

$$\frac{\partial \varepsilon_T}{\partial t} + \frac{1}{V_F}(u A_x \frac{\partial \varepsilon_T}{\partial x} + \nu A_y \frac{\partial \varepsilon_T}{\partial x} + w A_z \frac{\partial \varepsilon_T}{\partial z}) = \frac{CDIS1}{k_T}(PT + CDIS .G) + Diff_l - CDIS2\frac{\varepsilon_T^2}{k_T} \quad (15)$$

Flow 3D Hydro calculates the mean values for the hydraulic parameters for each cell using staggered grid system.

The Volume of Fluid (VOF) method was employed for the estimation of water surface within the context of this study.

The VOF method relies on the fraction α function as an indicator as presented in the Eq. (16), allowing the determination of the proportion of a computational cell filled with water, air, or a combination of both.

The software implementation utilizes the Tru-VOF method for accurately tracking the interface between water and air.

The VOF equation for interface tracking is expressed as follows Eq. (16):

$$\frac{\partial \alpha}{\partial t} + u_i \frac{\partial \alpha}{\partial x_i} = 0 \quad (16)$$

2.7 Implementation of Boundary and Initial Conditions

In the numerical solution, standard boundary conditions were implemented as follows:

At the inlet, the head discharge was specified for each case using condition P (specified pressure), which represents the pressure in meters and corresponds to the elevation of the fluid at the inlet.

For the lateral walls, the condition S (symmetry) was applied, indicating either no specific conditions to check on these walls or that the calculations were based on a control volume approach.

The bottom wall was set to the condition W (wall), indicating that it represents a solid surface through which the fluid flows. The top wall was set to atmospheric pressure.

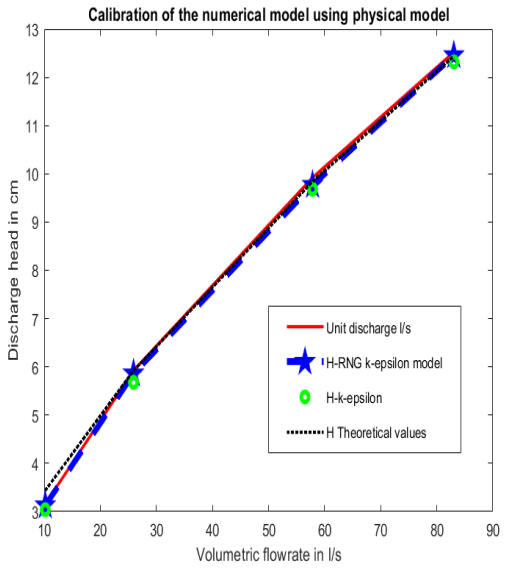

Fig. 5 Calibration of the numerical solution using physical model

The outflow condition, denoted by O (outflow), was applied to allow fluid to discharge and prevent water from accumulating in the domain.

Additionally, for the initial condition, water level at t=0 was specified.

3 RESULTS

3.1 Calibration of the Model

Employing a sensitivity analysis with empirical, numerical, and two turbulence models, alongside values from a physical model, the accuracy of the methods employed in this study were verified.

The analytical relationship (Reclamation, 1987) between the flow discharge and head discharges is provided by the Eq. (17):

$$Q = CLH^{\frac{3}{2}} \tag{17}$$

According to Fig. 5 and Tables 4, 5 the results indicate close agreement among the methods, ranging from nappe flow to skimming flow.

Notably, the turbulence model RNG $k-\varepsilon$ demonstrates a commendable alignment with the physical model in terms of the tested flow discharges.

Table 4 Comparison of the head discharges between experimental data and CFD

Q(l/s)	H-RNG $k-\varepsilon$ (cms)	H- $k-\varepsilon$ (cms)	H-Emp (cms)	H-Exp (cms)
10.2	3.16	3.128	3.04	3.44
25.9	5.92	5.86	5.68	5.92
58	9.92	9.76	9.68	9.84
83	12.52	12.46	12.32	12.44

Table 5 Comparison of relative mean error RME of the head discharges

Q(l/s)	RME H-RNG $k-\varepsilon$ (%)	RME $k-\varepsilon$ (%)
10.2	8.27	9.11
25.9	0.02	1.01
58	-0.63	0.75
83	-0.61	-0.13

The examination of the results of the Table 5 shows the maximum relative mean error RME between the experimental values and numerical values for both turbulence model (RNG $k-\varepsilon$, $k-\varepsilon$).For nappe flow regimes, the discrepancies between the two turbulence models and experimental data range from 8% to 9%. However, for high flow discharge conditions, when the skimming flow regime is prevalent, the differences are smaller, ranging from 1% to 0.13%.

Overall, RME does not exceed 10 % and become smaller for high flow discharges.

In addition, we conclude the performance of the H-RNG $k-\varepsilon$ is better than $k-\varepsilon$ turbulence model.

Both turbulence models yield satisfactory results, yet the RNG $k-\varepsilon$ model exhibits superior accuracy when compared to experimental data. This enhanced performance can be attributed to specific enhancements in the RNG $k-\varepsilon$ model. Notably, this model incorporates modifications not only in the constants of the transport equations but also introduces an additional term in the source term of the ε equation, leading to improved predictive capabilities.

3.2 Transition Zone with Ogee Crested Weir

Figure 6 illustrates a water surface diverging significantly and deviating from the profile of the steps within the transition zone connecting the ogee crest to the chute spillway. Notably, shock waves are observed in this region.

The initial configuration without steps can create dangerous hydraulic problems for the long-term operation of the structure;

Therefore, we chose to adjust the profile to ensure that the water profile conforms to the shape of the transition zone, aiming to prevent hydraulic dysfunction such as cavitation and shock waves (Reinauer & Hager, 1996, 1997; Souli et al., 2023a, b).

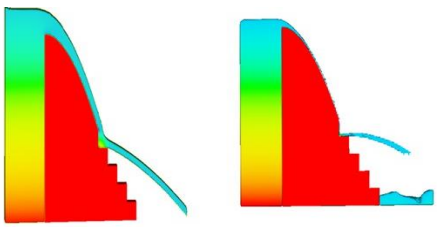

(a) (b)

Fig. 6 Flow over ogee crest for discharge (a) Q=25.9l/s (skimming flow), (b) Q=10.2 l/s (Nappe flow)

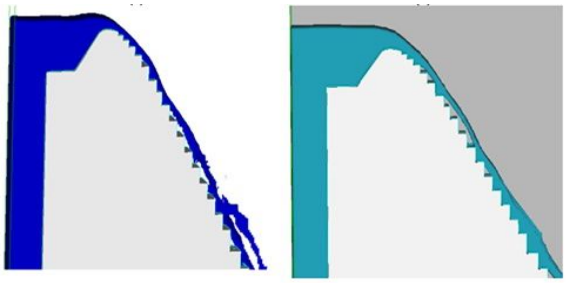

(a) (b)

Fig. 7 Flow over the modified profile for discharge (a) Q=10.2 l/s (Nappe flow), (b) Q=25.9 l/s (skimming flow)

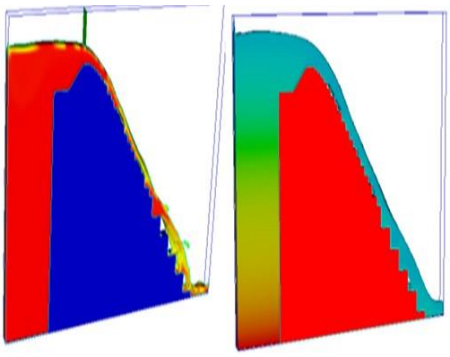

(a) (b)

Fig. 8 Flow over the modified profile for discharge (a) Q=58 l/s, (b) Q=83 l/s (Skimming flow)

3.3 Modelling the Modified Profile

In this part, the focus will be on the conditions upstream the stepped chute (in the transition zone between the weir and stepped chutes in the modified profile), the velocity distribution and the energy dissipation.

The results from the physical model, depicted in Fig. 9, demonstrate strong agreement with the numerical solutions, as illustrated in Figs. 7 and 8, regarding flow patterns and behavior.

The comparison between the results obtained from the numerical simulation and the physical model demonstrates consistent patterns. Validation of our numerical approach is achieved through Fig. 9, indicating that after modifying the profile in the critical zone (CZ), no jumps or shock waves occur in this region. The water surface conforms to the desired weir profile without any disturbances, aligning with the objectives of this study. This alignment between the physical and numerical models underscores the effectiveness of the modified profile in achieving the desired flow characteristics.

The Fig.6 represents the inflow conditions for flow discharges ranging from 10.2 l/s to 25.9 l/s in both numerical and physical models.

A noteworthy observation is the strong agreement between numerical approaches and experimental data.

Fig. 9 Validation of the Modified profile using the physical modeling (Skimming flow).

The mitigation of the spray zone effect is evident with the use of the modified profile, as confirmed by the physical modeling results, particularly in nappe flow. Furthermore, these outcomes affirm the numerical solution's capability to accurately capture the free surface in the CZ, effectively avoiding the springboard effect associated with our modified profile.

3.4 Comparison of Velocity Distribution

In this segment of our investigation, we presented in Fig. 10 a velocity distribution within the (CZ). The velocity profile as a function of $Z = \frac{y_c}{z}$ was graphically represented to gain a comprehensive understanding of the impact of introducing additional steps in the CZ.

This allowed us to compare the velocity fields for the tested cases through both numerical and physical modeling, facilitating a thorough examination of the effects of varying step configurations on the flow dynamics.

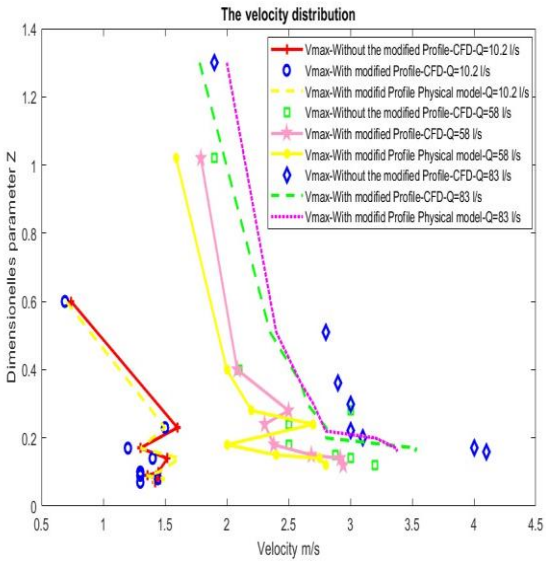

Fig. 10 Velocity distribution for the tested cases and comparison with the physical model

As depicted in Fig.10, which illustrates the dimensionless parameter Z as a function of velocity, the velocity in nappe flow exhibits fluctuations with the Z parameter. Initially, at the beginning of the weir profile where z is small (z-axis), the velocity, measured and calculated, is less than 0.5 m/s, a result confirmed by experimental data. Moving along the z-axis of the profile, the velocity distribution shows two maximum velocity values exceeding 1.5 m/s. This velocity distribution is valid for nappe flow, as the water surface impacts the steps without a pseudo bottom surface, typical of skimming flow. The overall pattern of the velocity distribution indicates rapid fluctuations between these two parameters.

For skimming flow with a discharge of 58 l/s, initial observations at the beginning of the weir profile, where z is small (z-axis), indicate a velocity less than 2 m/s, a finding validated by the physical model. Progressing along the z-axis, the velocity distribution reveals several maximum velocity values exceeding 2.5 m/s. A comparison with the variant of the profile without modifications shows a velocity decrease of 0.2 m/s, confirming the effectiveness of the modified profile. The variation of the velocity with the Z parameter demonstrates sharp changes with fluctuations at various points along the z-axis.

For a discharge of 83 l/s, the velocity distribution differences between the tested profiles are more pronounced, with an overall increase of 0.7 m/s. Initially, at the beginning of the weir, velocities exceed 3 m/s. As Z ranges from 0 to 0.4, both numerical and physical models with the modified profile exhibit similar values. Beyond Z=0.4, an asymptotic value is observed in both approaches, with a gradual deviation by an average of 0.1 m/s between them.

As indicated in the Fig. 10 for the nappe flow regime at Q=10.2 l/s, the modified profile significantly contributes to reducing the velocity, showing a crucial role. It leads to a 10 % velocity reduction compared to the CEDEX profile and an even more substantial reduction of over 18 % when compared to a scenario with only the ogee-crested weir in the Critical CZ.

This significant impact is attributed to the addition of steps; the flow adheres to these steps, facilitating energy dissipation, especially for lower flow discharges where the flow jumps over multiple steps.

As depicted in the Fig. 10, during the skimming flow regime at Q=58-83 l/s, the modified profile plays a significant role in reducing velocity, demonstrating its crucial impact. It results in a 7% reduction in velocity compared to the CEDEX profile presented in the Fig. 11 as example of the outputs of the numerical methods. Moreover, even more substantial reduction of over 15% when contrasted with the profile of ogee-crested weir in the CZ shown in the Fig. 6. Notably, both flow discharges exhibit similar trends, and values with the modified profile closely align with those obtained from experimental data.

Overall, it is evident that the modified profile demonstrates favorable performance in terms of reducing velocity within the Critical CZ across various flow discharges.

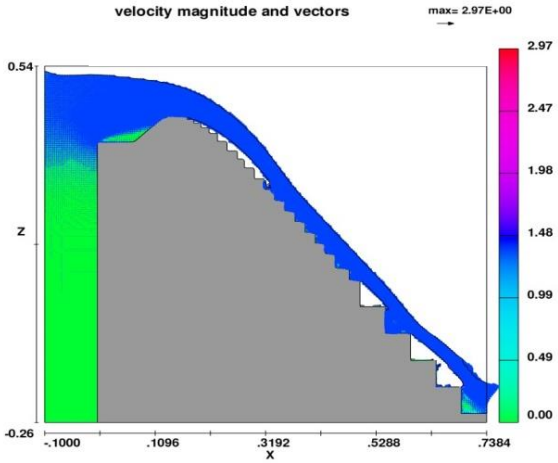

Fig. 11 Example of simulation of the CZ-CEDEX profile

3.5 The Dissipation Rate: Physical and Numerical Approaches

In order to compute the residual energy at the bottom of the stepped chute, the conjugate depth y_2 was measured in the physical model, with the help of the control section downstream the stepped spillway, and then y_1 was computed with the help of the Eq. 18 of the hydraulic jump:

$$y_1 = \frac{y_2}{2}(-1+\sqrt{1+8Fr_2^2}) \tag{18}$$

Water velocity and heights in the stilling basin were also measured. which enabled us to compute the Froude number, ensuring subcritical flow downstream of the hydraulic jump. Additionally, we utilized the Flow-3D Hydro software to visually track the development of the hydraulic jump. The accuracy of these measurements was further confirmed through validation with experimental data.

3.6 Comparison of the Energy Dissipation

Figure 12 illustrate the relation between flow rate (Q) and dissipation rate, in both scenarios, one with the altered profile in the critical zone (CZ) and one without. In this section, our objective is to investigate the impact of modifying the profile in the critical zone (CZ), varying the number of steps, and adjusting the volume flow rate during the transition from nappe flow to skimming flow. This exploration is conducted using the empirical Eq. (5) previously mentioned, alongside experimental data and numerical approaches.

In nappe flow, as emphasized in the introduction, the dissipation rate is notably high due to the formation of hydraulic jumps at each step, resulting in increased dissipation for smaller flow discharges. As illustrated in Fig.13 for a range of steps (N=16 to 60), the dissipation rate without the modified profile ranges from 93% to 97%, whereas without the modification, it varies between

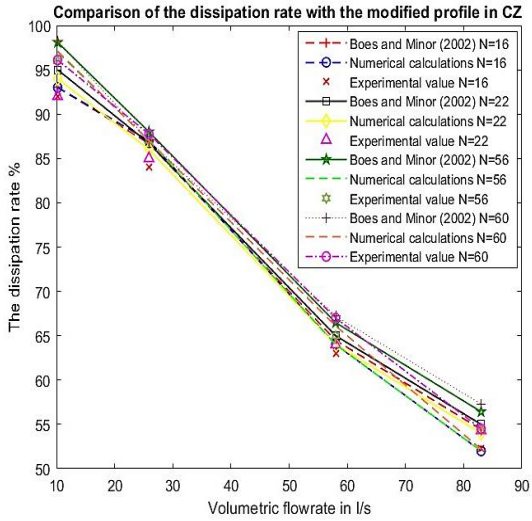

Fig. 12 Dissipation rate: The modified profile

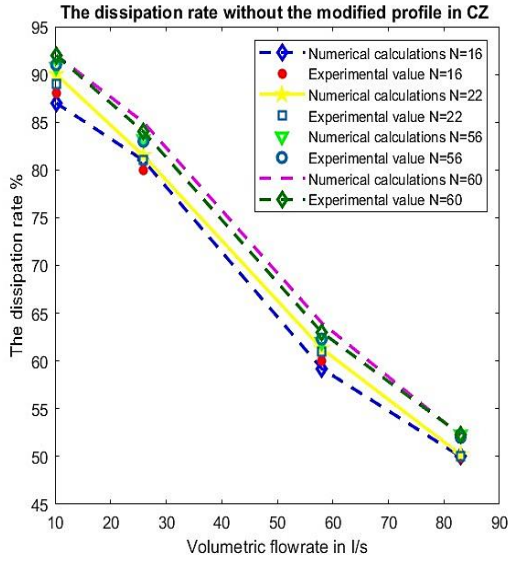

Fig. 13 Dissipation rate: Without the Modified profile

88% and 92%. This signifies that the modified profile contributes an additional 5% or more to the dissipation rate—a critical parameter in stepped spillways.

The modified profile facilitates enhanced water-surface adherence to the critical zone (CZ), allowing increased friction with the steps compared to the scenario without the proposed profile.

As observed in Fig.13, there is a clear trend of decreasing dissipation rate as the flow rate increases. This phenomenon is attributed to the skimming flow regimes, where the flow exhibits a distinctive parallel water surface, avoiding direct impact on the steps as seen in nappe flow regimes. Instead, the flow forms cavities in the corners of each step, aerating the flow and mitigating the impact of the steps. Additionally, the dissipation rate rises with an increase in the number of steps. Notably, the modified profile demonstrates a significant impact, enhancing with over 4% to the dissipation rate.

Furthermore, the precision of the numerical outcomes aligns well with the experimental data, as shown in Figs7, 8, 9. The relative mean error across all tested cases remains below 3%. This signifies the effectiveness of the sensitivity analysis conducted on the mesh grid and turbulence model employed which is a crucial preliminary step for ensuring reliable results.

4 Conclusion

In this paper, we have addressed the challenges associated with the initial design of stepped spillways using an ogee crest and CEDEX profile, which led to issues such as jumps and impingement in the transition zone. To address these challenges, we proposed modifications to the profile, including extending the initial tangential point (from T to T') and adopting width as a function of the head discharge until the stepped chute, as well as incorporating additional steps in the critical zone (CZ).

The validation of our numerical approach was conducted using various physical models with different profiles and numbers of steps. Our results demonstrate that the modified profile yields reliable results across all flow regimes in the stepped spillway, with a notable reduction in velocity by over 7% and an improvement in the dissipation rate by more than 4%.

Furthermore, the calculated relative mean error for energy dissipation and velocity between physical and numerical solutions remains below 10%, indicating the feasibility of using CFD methods to compute energy dissipation accurately.

For future research, we recommend exploring the sensitivity to different slopes (the ratio h/l) and studying the pressure distribution in the critical zone using the modified profile. In addition, investigating the effect of roughness on the critical zone would be beneficial for further understanding and improving the design of stepped spillways.

Acknowledgements

The completion of this research work would not have been possible without the generous support and valuable contributions from the Moroccan hydraulic Laboratory and Hassania School of Public Works. Their expertise and resources have significantly enriched the quality of this study.

Conflict of Interest

The authors declare that they have no known competing financial interests or personal relationships that could have appeared to influence the work reported in this paper.

AUTHORS CONTRIBUTION

H. Souli: Investigation, Software, Validation, Conceptualization, Methodology, Writing original draft, Visualization. **J. Ahattab**: Investigation, Visualization,

Supervision, Writing, Review & editing. **S. Bensallam**: Investigation, Supervision, Review & editing

REFERENCES

AlTalib, A. N., Mohammed, A. Y., & Hayawi, H. A. (2019). Hydraulic jump and energy dissipation downstream stepped weir. *Flow Measurement and Instrumentation*, *69*, 101616. https://doi.org/10.1016/j.flowmeasinst.2019.101616

Baylar, A., Emiroglu, M. E., & Bagatur, T. (2006). An experimental investigation of aeration performance in stepped spillways. *Water and Environment Journal*, *20*(1), 35-42. https://doi.org/10.1111/j.17476593.2005.00009.x

Bayon, A., Valero, D., García-Bartual, R., & López-Jiménez, P. A. (2016). Performance assessment of OpenFOAM and FLOW-3D in the numerical modeling of a low Reynolds number hydraulic jump. *Environmental Modelling & Software*, *80*, 322-335. https://doi.org/10.1016/j.envsoft.2016.02.018

Boes, R. M. (2020). *Scale effects in modelling two-phase stepped spillway flow*. Hydraulics of stepped spillways. CRC Press. https://doi.org/10.1201/9781003078609-10

Boes, R. M., & Hager, W. H. (2003a). Hydraulic design of stepped spillways. *Journal of Hydraulic Engineering*, *129*(9), 671-679. https://doi.org/10.1061/(ASCE)07339429(2003)129:9(671)

Boes, R. M., & Hager, W. H. (2003b). Two-phase flow characteristics of stepped spillways. *Journal of Hydraulic Engineering*, *129*(9), 661-670. https://doi.org/10.1061/(ASCE)07339429(2003)129:9(661)

Boes, R. M., & Hager, W. H. (2003c). Two-phase flow characteristics of stepped spillways. *Journal of Hydraulic Engineering*, *129*(9), 661-670. https://doi.org/10.1061/(asce)0733-9429(2003)129:9(661)

Chanson, H. (2001). Hydraulic design of stepped spillways and downstream energy dissipators. *Dam Engineering*, *11*(4), 205-242. https://doi.org/10.1061/(asce)hy.1943-7900.0001107

Chanson, H., & Gonzalez, C. A. (2005). Physical modelling and scale effects of air-water flows on stepped spillways. *Journal of Zhejiang University-Science A*, *6*(3), 243-250. https://doi.org/10.1631/BF02872325

Dalili Khanghah, K., & Kavianpour, M. R. (2020). Numerical investigation of the effect of CEDEX profile on the hydraulic parameters in the stepped spillway and the performance of this profile in various chute slopes. *Iranian Journal of Science and Technology, Transactions of Civil Engineering*, *44*(4), 1247-1254. https://doi.org/10.1007/s40996-019-00313-8.https://doi.org/10.1007/s40996-019-00313-8

Daneshfaraz, R., Kaya, B., Sadeghfam, S., & Sadeghi, H. (2014). Simulation of flow over ogee and stepped spillways and comparison of finite element volume and finite element methods. *Journal of Water Resource and Hydraulic Engineering*, *3*(2), 37-47.

Daneshfaraz, R., Sadeghi, H., Ghaderi, A., & Abraham, J. P. (2024a). Characteristics of hydraulic jump and energy dissipation in the downstream of stepped spillways with rough steps. *Flow Measurement and Instrumentation*, *96*, 102506. https://doi.org/10.1016/j.flowmeasinst.2023.102506

Daneshfaraz, R., Sadeghi, H., Ghaderi, A., & Abraham, J. P. (2024b). The effect of gabion steps on the hydraulic jump characteristics downstream of stepped spillways. *Water Science*, *38*(1), 128-139. https://doi.org/10.1080/23570008.2024.2307243

Ghaderi, A., Daneshfaraz, R., Torabi, M., Abraham, J., & Azamathulla, H. M. (2020). Experimental investigation on effective scouring parameters downstream from stepped spillways. *Water supply*, *20*(5), 1988-1998. https://doi.org/10.2166/ws.2020.113

Hager, W. H., Schleiss, A. J., Boes, R. M., & Pfister, M. (2020). *Hydraulic engineering of dams*. CRC Press. https://doi.org/10.1201/9780203771433

Kaheh, M., Kashefipour, S. M., & Dehghani, A. (2014). *Comparison of k–ε and RNG k–ε turbulent models for estimation of velocity profiles along the hydraulic jump on corrugated beds.* 6th International symposium on environmental hydraulics, LAHR. Athens, Greece.

Khatsuria, R. M. (2004). *Cavitation in Spillways and Energy Dissipators*. *Hydraulics of Spillways and Energy Dissipators* (p. 541-568). CRC Press.

Mateos Iguacel, C., & Elviro Garcia, V. (1995). *Stepped spillways. Design for the transition between the spillway crest and the steps.* Proceedings Of The Congress-International Association For Hydraulic Research, 1, 260-265. https://doi.org/10.1201/9781003078609-15

Ohtsu, I., Yasuda, Y., & Takahashi, M. (2004). Flow characteristics of skimming flows in stepped channels. *Journal of Hydraulic Engineering*, *130*(9), 860-869. https://doi.org/10.1061/(ASCE)07339429(2004)130:9(860)

Pletcher, R. H., Tannehill, J. C., & Anderson, D. (1997). *Computational fluid mechanics and heat transfer*. CRC press. https://doi.org/10.1201/b12884

Quintela, A. C. (1980). *Flow aeration to prevent cavitation erosion.* Water Power Dam Constr.;(United Kingdom), 32(1).

Rajaratnam, N. (1990). *Skimming flow in stepped spillways. Journal of Hydraulic Engineering*, *116*(4), 587-591.

https://doi.org/10.1061/(asce)0733-9429(1990)116:4(587)

Reclamation, U. S. B. of. (1987). *Design of small dams*. US Department of the Interior, Bureau of Reclamation.

Regan, R. P., Munch, A. V., & Schader, E. K. (1979). *Cavitation and erosion damage of sluices and stilling basins at two high-head dams*. Proceedings of 13th ICOLD Congress, New Delhi Q, 50, 177-198.

Reinauer, R., & Hager, W. H. (1996). Shockwave in air-water flows. *International journal of multiphase flow*, *22*(6), 1255-1263. https://doi.org/10.1016/0301-9322(96)00049-3

Reinauer, R., & Hager, W. H. (1997). Supercritical bend flow. *Journal of Hydraulic Engineering*, *123*(3), 208-218. https://doi.org/10.1061/(asce)0733-9429(1997)123:3(208)

Souli, H., Ahattab, J., & Agoumi, A. (2023a). Hydraulic study of fan spillway using computational fluid dynamics (CFD) and Experimental Approaches. In K. Baba, L. Ouadif, A. Nounah & M. Bouassida (Éds.), *Advances in research in geosciences, geotechnical engineering, and environmental science* (p. 443-453). Springer Nature Switzerland. https://doi.org/10.1007/978-3-031-49345-4_42

Souli, H., Ahattab, J., & Agoumi, A. (2023b). Investigating supercritical bended flow using physical model and CFD. *Modelling and Simulation in Engineering*, *2023*, 5542589. https://doi.org/10.1155/2023/5542589

Takahashi, M., Yasuda, Y., & Ohtsu, I. (2001). Energy dissipation of skimming flows on stepped channels. *Proceedings of Hydraulic Engineering*, *45*, 415-420. https://doi.org/10.2208/prohe.45.415